inter.noise
27-30 AUGUST HONG KONG 2017

# Analogue Transformation Acoustics in Aeronautics

Umberto IEMMA[1] and Giorgio PALMA[2]
Roma Tre University, Department of Engineering, Rome, Italy

## ABSTRACT

The objective of the paper is a critical review within the context of aeronautical applications of the Analogue Transformation Acoustics (ATA) approach for the modelling of acoustic metamaterials. The ATA approach has been introduced to overcome the limitation of the metamaterials design methods based on the Standard Transformation Acoustics (STA) imposed by the requirement of a strict formal invariance of the governing equations. Indeed, in case of acoustic perturbations propagating within moving media, the convective terms are responsible of the failure of formal invariance under the action of conformal mappings as a consequence of the combination of space and time derivatives. The ATA is based on the concept of analogue spacetimes and fully relies on the analytical tools of Lorentzian differential geometry. The great advantages of the method is the possibility to handle a background flow, conversely to the STA which fails in presence of convection. Despite the undoubted appeal of this feature in the eyes of an aeroacoustician, its potential has not been completely disclosed yet. The class of transformations that yield a physically meaningful aerodynamics in the virtual analogue spacetime has not been explored in details, preventing the application of the method in aeronautics. The present paper analyses the relationship between the the analogue velocity field with a realistic potential flow. The analytical comparison is validated through numerical simulations of two classic benchmarks: the irrotational flow of an inviscid, incompressible fluid around a circular cylinder and the flow through a bumped wall. The target acoustic behaviour is the cancellation of the scattering (cloaking) induced by the cylinder and the bump.

Keywords: metamaterials, cloaking, ATA, transformation acoustics.

## 1 INTRODUCTION

Since the achievement of electromagnetic invisibility of objects by Pendry *et al.*(1) and the subsequent porting by Cummer and Schurig (2) of the concept and methodology to acoustics, based on the observation about the formal analogy between mass and momentum equations for an inviscid fluid at rest under small pressure perturbation and the single polarization Maxwell's equations introducing a suitable variables exchange, an extensive literature has been produced on the topic. Most of the research activity has focused on the achievement of acoustic invisibility, or cloaking, *i.e.* the total abatement of the scattering effects induced by an obstacle impinged by an acoustic perturbation. The standard approach (Standard Transformation Acoustics) imported from electromagnetism involves the exploitation of governing equations formal invariance under coordinates transformations and the reinterpretation of the arising coefficients as mechanical properties of an ideal material, or metamaterial, suitable to obtain the desired modification of the scattered field. The concept of acoustic metamaterial has disclosed an incredible potential of development for breakthrough technologies. Unfortunately, the extension of the same concepts to aeroacoustics has turned out to be not a trivial task, because of the different structure of the governing equations, characterized by the presence of the background

[1]umberto.iemma@uniroma3.it
[2]giorgio.palma@uniroma3.it

aerodynamic convection. The latter introduces transport terms in the governing equations which yield, under suitable assumptions, the convective forms of the wave operator. The arising mixed space–time derivatives make the formal invariance of the governing equations under coordinate transformations to be lost.

Recently, Garcia–Meca et al. (3–7), aiming to overcome this main limitation of the STA, proposed an innovative approach called Analogue Transformation Acoustic. Starting from the observation, first published by Visser (8), that the convective form of the wave equation has a relativistic structure, this new technique uses the existence of such an auxiliary abstract relativistic system to build an analogue spacetime on which operates and searches for relativistic analogues of laboratory phenomena. The appealing feature of the method for aeroacoustic applications lies in the possibility to handle a background aerodynamic flow (on which the acoustic perturbation travels) transforming it together with the spacetime. However its potential in this field has just sketched in the work of the group (5, 6) and not explored in details.

Till now, in fact, the applications of ATA in the aeroacoustic field are limited to the cloaking of a small geometric irregularity on a flat wall, the so called *carpet cloaking*, using a numerically obtained quasi-conformal transformation as described in (9, 10). After a brief review of the ATA, addressed in Section 2, and its application on the cited case in Section 3.1, the methodology is extended in Section 3.2 to consider the cloaking of a cylinder immersed in a moving hosting fluid. Efficiency of the proposed design methodology is investigated in Section 4. The present paper tries then, in Section 5, to shed light on the physical meaning of the velocity fields resulting from the application of the ATA methodology in combination with quasi–conformal transformations and their relationship with potential flows.

## 2 ANALOGUE TRANSFORMATION ACOUSTICS SUMMARY

The Analogue Transformation Acoustics was first presented in 2012 by Garcia-Meca and his research group (3), as a new framework for acoustic metamaterials design, alternative to the standard transformation acoustics, and successively developed in (4–7). In this paper just a brief review of the methodology and its application is presented, whereas for exhaustive details the reader is referred to the previously mentioned works addressed in the bibliography.

The ATA methodology starts considering the equation for the acoustic potential in a barotropic inviscid and irrotational fluid to model the sound propagation inside such media

$$-\frac{\partial}{\partial t}\left(\frac{\rho}{c^2}\left(\frac{\partial\phi}{\partial t}+\mathbf{v}\cdot\nabla\phi\right)\right)+\nabla\cdot\left(\rho\nabla\phi-\frac{\rho}{c^2}\left(\frac{\partial\phi}{\partial t}+\mathbf{v}\cdot\nabla\phi\right)\mathbf{v}\right)=0 \tag{1}$$

This equation can be written in a very elegant way for arbitrary spatial coordinates, showing, as noted by Visser (8), a Lorentzian metric

$$\partial_\mu\left(f^{\mu\nu}\partial_\nu\phi\right)=0 \tag{2}$$

with

$$f^{\mu\nu}=\frac{\rho}{c^2}\begin{pmatrix} -1 & \vdots & -v^j \\ \cdots & \cdot & \cdots \\ -v^i & \vdots & c^2\gamma^{ij}-v^iv^j \end{pmatrix} \tag{3}$$

Equation 2 can be written as a D'Alambertian of a scalar field in a curved Lorentzian (or *pseudo-Riemannian*) manifold:

$$\frac{1}{\sqrt{-g}}\frac{\partial}{\partial\mu}\left(\sqrt{-g}g^{\mu\nu}\frac{\partial\phi}{\partial\nu}\right)=0 \tag{4}$$

provided that the contravariant metric tensor is given by

$$\sqrt{-g}g^{\mu\nu} = f^{\mu\nu} \qquad (5)$$
$$g = \det(g_{\mu\nu})$$

The ATA exploits the relativistic structure and symmetries of Eq. 4, which is related to the classical sound propagation equations that are, instead, non-relativistic, hence enabling the use of generic coordinate transformations mixing space and time

$$f : x^\mu \to \bar{x}^{\bar{\mu}} = \Lambda^{\bar{\mu}}_{\nu} x^\nu \qquad (6)$$

to deform the space-time in any chosen way. It is evident how the considered metric depends on the medium parameter.

The procedure, described in the cited papers, to obtain ATA-designed metamaterials can be summarized as follows:

- Eq 2 is written in a physical and simple coordinate system, and a *virtual* (inverse) metric is defined.

$$g^{\mu\nu} = \frac{1}{\rho_V c_V} \begin{pmatrix} -1 & \vdots & -v_V^j \\ \cdots & \cdot & \cdots \\ -v_V^i & \vdots & c_V^2\gamma_V^{ij} - v_V^i v_V^j \end{pmatrix} \qquad (7)$$

- A desired general coordinate transformation $\bar{x}^{\bar{\mu}} = f(x^\mu)$ can be applied to Eq. 2, to write it into a new virtual space-time with a new metric $\bar{g}$ obtained by standard tensorial transformation rule

$$\bar{g}^{\bar{\mu}\bar{\nu}} = \Lambda^{\bar{\mu}}_{\mu}\Lambda^{\bar{\nu}}_{\nu} g^{\mu\nu} \qquad (8)$$

- A second *real* medium with its parameter $\rho_R$, $c_R$, $v_R$, is considered with its metric $\tilde{g}^{\tilde{\mu}\tilde{\nu}}$, and finally the formal invariance of Eq. 4 is exploited, which implies

$$\sqrt{-\bar{g}}\bar{g}^{\bar{\mu}\bar{\nu}} = \sqrt{-\tilde{g}}\tilde{g}^{\tilde{\mu}\tilde{\nu}} \qquad (9)$$

with

$$\bar{g}^{\bar{\mu}\bar{\nu}} = \frac{1}{\bar{\rho}_V \bar{c}_V} \begin{pmatrix} -1 & \vdots & -\bar{v}_V^j \\ \cdots & \cdot & \cdots \\ -\bar{v}_V^i & \vdots & \bar{c}_V^2\bar{\gamma}_V^{ij} - \bar{v}_V^i \bar{v}_V^j \end{pmatrix}, \quad \tilde{g}^{\tilde{\mu}\tilde{\nu}} = \frac{1}{\tilde{\rho}_R \tilde{c}_R} \begin{pmatrix} -1 & \vdots & -\tilde{v}_R^j \\ \cdots & \cdot & \cdots \\ -\tilde{v}_R^i & \vdots & \tilde{c}_R^2\tilde{\gamma}_R^{ij} - \tilde{v}_R^i \tilde{v}_R^j \end{pmatrix} \qquad (10)$$

From Eq. 9 one can obtain the relation between the material parameters of the virtual and the new real media, able to reproduce the effect of the coordinate change, equalling each element of the two matrices.

Since Eq. 1 is not able to take into account anisotropy, the coordinate transformation that can be used within the ATA framework are limited to spatially conformal transformations, known to produce isotropic material parameters (provided that the starting medium is also isotropic as in the usual cases). In (5) is specified that, in presence of a background velocity field, this should be modified following the transformation imposed, satisfying Eq. 9

$$\tilde{v}_R^i = \bar{v}_V^{\bar{i}} = \Lambda^{\bar{i}}_i v_V^i \qquad (11)$$

However, the same result can be obtained just equalling each term of Eq. 10, following the described procedure.

## 3 NUMERICAL SIMULATIONS

Two test cases are presented in the following: the carpet cloaking of a bumped wall and the cloaking of a cylinder. In both cases a background uniform velocity field is present and ATA methodology is applied to design a proper cloaking device. All simulations are performed using a commercial finite element software (COMSOL Multiphysics).

### 3.1 Carpet cloaking

In (5) is presented an application of the method, described in Section 2, to the case of the carpet cloaking of a bump on a flat wall, in presence of a uniform mean flow parallel to the wall having velocity $\mathrm{v_V}$ = 120 (m/s), *i.e.* Mach number $\mathrm{M_V}$ = 0.35. The shape of the bumped wall is defined by (18) (all dimensions expressed in meters)

$$\begin{cases} y = 0.2\,\cos^2(\pi x/2) & 1 \leq x \leq 3, \\ y = 0 & \text{otherwise} \end{cases} \tag{12}$$

The metamaterial is positioned in a rectangular area $\mathcal{D}_\mathrm{c}$, surrounding the bump, 1.5 m high and 4 m long. Applying the method described in (9), a quasi–conformal transformation is obtained numerically, so that the bumped–space is mapped in a flat–space, where the first corresponds to the deformed virtual space of the ATA approach, whereas the latter is the starting physical space. This method consists in solving the Laplace's equation imposing suitable boundary conditions that specify the behaviour required by the transformation. Specifically, the equation solved are

$$\bar{\nabla}^2 y = 0, \qquad y \in \mathcal{D}_\mathrm{c} \tag{13}$$

$$\text{with b.c.}$$

$$\begin{aligned} y(\bar{a}) &= 0, & y(\bar{b}) &= \bar{b} = b \\ \frac{\partial y}{\partial \bar{n}}(\bar{c}) &= 0, & \frac{\partial y}{\partial \bar{n}}(\bar{d}) &= 0 \end{aligned}$$

and

$$\bar{\nabla}^2 x = 0, \qquad x \in \mathcal{D}_\mathrm{c} \tag{14}$$

$$\text{with b.c.}$$

$$\begin{aligned} x(\bar{c}) &= \bar{c} = c, & x(\bar{d}) &= \bar{d} = d \\ \frac{\partial x}{\partial \bar{n}}(\bar{a}) &= 0, & \frac{\partial x}{\partial \bar{n}}(\bar{b}) &= 0 \end{aligned}$$

where the $\bar{\nabla}^2$ denotes the differentiation in the virtual space, *i.e.* the bumped–space, and $\bar{\mathrm{a}}$, $\bar{\mathrm{b}}$, $\bar{\mathrm{c}}$ and $\bar{\mathrm{d}}$ are defined in Figure 1. Solving Eqs. 13 and 14 one numerically obtains $x = f_1(\bar{x}, \bar{y})$ and $y = f_2(\bar{x}, \bar{y})$ inside $\mathcal{D}_\mathrm{c}$, as shown in Fig. 1. From this solution is possible to derive the design parameters of the desired metamaterial. The coordinate transformation results to be quasi–conformal and it is able to minimize the anisotropy required from the metamaterial, as demonstrated in (9), so that it can be neglected, jelding to an isotropic device. Using the properties of conformal transformation, in fact, we have that $\frac{\partial x}{\partial \bar{x}} = \frac{\partial y}{\partial \bar{y}}$ and $\frac{\partial x}{\partial \bar{y}} = -\frac{\partial y}{\partial \bar{x}}$, and the inverse transformation matrix can be written as

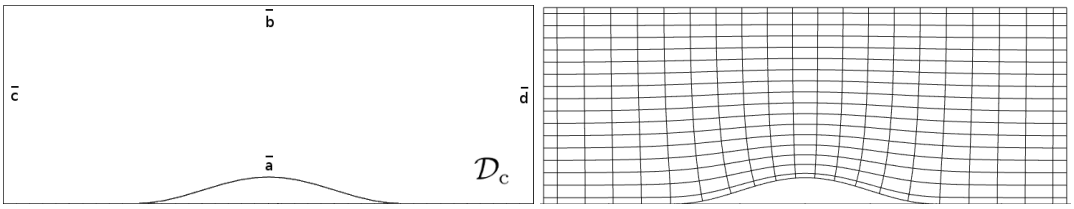


Figure 1 – Carpet cloaking: bumped wall geometry and boundary definitions and coordinate transformation: $x = f_1(\bar{x}, \bar{y})$ and $y = f_2(\bar{x}, \bar{y})$

$$\Lambda^{\mu}_{\bar{\mu}} = \begin{pmatrix} 1 & 0 & 0 & 0 \\ 0 & \frac{\partial x}{\partial \bar{x}} & \frac{\partial x}{\partial \bar{y}} & 0 \\ 0 & \frac{\partial y}{\partial \bar{x}} & \frac{\partial y}{\partial \bar{y}} & 0 \\ 0 & 0 & 0 & 1 \end{pmatrix} = \begin{pmatrix} 1 & 0 & 0 & 0 \\ 0 & \frac{\partial y}{\partial \bar{y}} & -\frac{\partial y}{\partial \bar{x}} & 0 \\ 0 & \frac{\partial y}{\partial \bar{x}} & \frac{\partial y}{\partial \bar{y}} & 0 \\ 0 & 0 & 0 & 1 \end{pmatrix} \tag{15}$$

and hence, the transformation matrix in Eq. 6 is

$$\Lambda^{\bar{\mu}}_{\mu} = \begin{pmatrix} 1 & 0 & 0 & 0 \\ 0 & \frac{\frac{\partial x}{\partial \bar{x}}}{\left(\frac{\partial x}{\partial \bar{x}}^2 + \frac{\partial x}{\partial \bar{y}}^2\right)} & \frac{\frac{\partial x}{\partial \bar{y}}}{\left(\frac{\partial x}{\partial \bar{x}}^2 + \frac{\partial x}{\partial \bar{y}}^2\right)} & 0 \\ 0 & \frac{\frac{\partial y}{\partial \bar{x}}}{\left(\frac{\partial x}{\partial \bar{x}}^2 + \frac{\partial x}{\partial \bar{y}}^2\right)} & \frac{\frac{\partial y}{\partial \bar{y}}}{\left(\frac{\partial x}{\partial \bar{x}}^2 + \frac{\partial x}{\partial \bar{y}}^2\right)} & 0 \\ 0 & 0 & 0 & 1 \end{pmatrix} \tag{16}$$

Following the procedure described in Section 2, real medium parameters can be obtained from Eq. 9 as

$$\begin{aligned} c_R &= \frac{c_V}{\sqrt{\frac{\partial x}{\partial \bar{x}}^2 + \frac{\partial x}{\partial \bar{y}}^2}} & \rho_R &= \rho_V \\ v_{Rx} &= \frac{v_{Vx}\frac{\partial x}{\partial \bar{x}} - v_{Vy}\frac{\partial x}{\partial \bar{y}}}{\sqrt{\frac{\partial x}{\partial \bar{x}}^2 + \frac{\partial x}{\partial \bar{y}}^2}} & v_{Ry} &= \frac{v_{Vx}\frac{\partial x}{\partial \bar{y}} + v_{Vy}\frac{\partial x}{\partial \bar{x}}}{\sqrt{\frac{\partial x}{\partial \bar{x}}^2 + \frac{\partial x}{\partial \bar{y}}^2}} \end{aligned} \tag{17}$$

The distribution of $\mathrm{c_R/c_V}$ is depicted in Fig. 2.

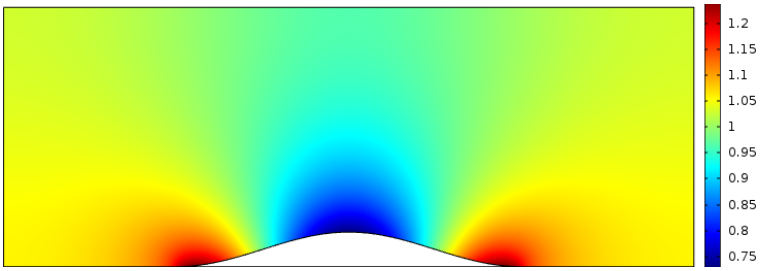


Figure 2 – Field distribution of $\mathrm{c_R/c_V}$

It is interesting to note how in a static case, *i.e.* $\vec{v}_v$ = 0, using the theoretical approach proposed by Norris (13) one obtains the same results that can be found applying the ATA method: in fact, it emerges that the bulk modulus of the metamaterial is $\mathcal{K}_R = J\mathcal{K}_V$, with $J = \det(\mathbf{\Lambda}) = \frac{1}{\sqrt{\frac{\partial x}{\partial \bar{x}}^2 + \frac{\partial x}{\partial \bar{y}}^2}}$, and the density is just a scalar matrix $\boldsymbol{\varrho}_R = J(\mathbf{\Lambda}\mathbf{\Lambda}^T)^{-1}\rho_0 = \mathbf{I}\rho_0$, confirming the equivalence of two approaches.

Fig. 3 shows the cloaking effect of the designed device in presence of a background: the acoustic fields associated to a Gaussian beam impinging from the left the flat wall, and the cloaked bump and the naked bump are compared; when the cloak is present, a small spatial shift of the reflected wave seems to appear compared to the free field simulation, but the wavefronts shape are indistinguishable from the flat wall.

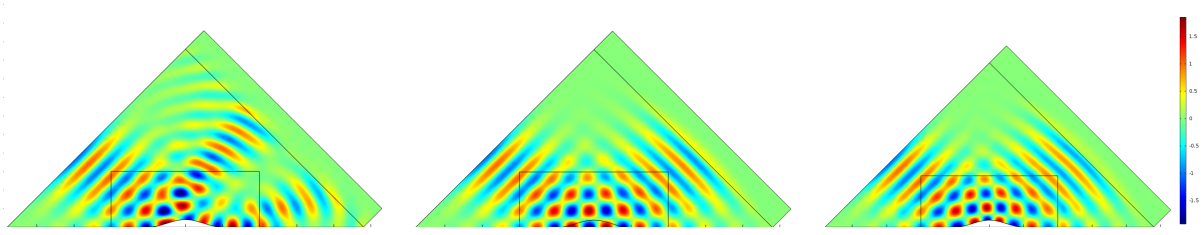

(a) Naked (b) Free Field (c) Cloaked

Figure 3 – Gaussian beam at 655 Hz impinging on a bumped wall (a), on a flat wall (b) and on a cloaked bump (c), field visualization of Real part of acoustic potential $\mathrm{Re}(\phi)$.

### 3.2 Acoustic cloaking of a cylinder

To the best of the authors knowledge, a conformal or quasi–conformal transformation has never been applied to obtain the abatement of the scattering from a body completely immersed in a moving fluid. The method described in the above Section for the determination of the coordinate mapping, and hence of the metamaterial parameters, introduces an approximation when neglects the anisotropy of the metamaterial: this means that we are assuming a quasi–conformal mapping to be a conformal mapping. This approximation holds clearly just by virtue of the small size of the obstacle introduced on the flat wall. Anisotropy, evidently, is going to increase with the height of the bump, the length being equal. Applying the method to a cylindrical object inside the fluid domain, this would no longer produce a conformal coordinate transformation, as can be seen from Fig. 4, hence the anisotropy of the metamaterial would no longer be negligible.

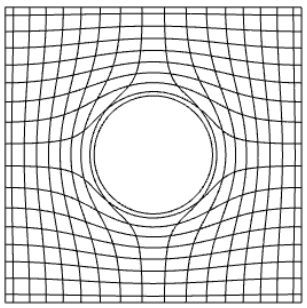

Figure 4 – Non–conformal mapping arising from application of method in (9)

The problem can be overtaken, slightly modifying the methodology used for the carpet cloaking case, at the price of losing the omnidirectionality of the cloaking. This should not be a critic issue as it would not affect the efficiency of the method in all those aeroacoustic applications where the relative position between source and scatterers is known a priori and invariant. We will examine the case presented in Fig. 5, the acoustic cloaking of a cylinder of radius r = 0.2 m, from the sound emitted by a point source in a moving fluid with background velocity $\mathrm{v_v}$ = 120 (m/s) ($\mathrm{M_v}$ = 0.35) parallel to x–axis, the cloaking device occupying a square region which side

length is $l_1 = 4$ m. The mapping is obtained solving just one Laplace's equation, corresponding to Eq. 13

$$\bar{\nabla}^2 y = 0, \qquad y \in \mathcal{D}_{\mathrm{c}} \tag{18}$$

$$\text{with b.c.}$$

$$y(\bar{a}) = 0, \qquad y(\bar{b}) = \bar{b} = b \qquad y(\bar{c}) = \bar{c} = c$$
$$\frac{\partial y}{\partial \bar{n}}(\bar{d}) = 0, \qquad \frac{\partial y}{\partial \bar{n}}(\bar{e}) = 0$$

with the $\bar{\nabla}^2$ denoting the differentiation in the virtual space, while $\bar{\mathrm{a}}$, $\bar{\mathrm{b}}$, $\bar{\mathrm{c}}$ and $\bar{\mathrm{d}}$ are defined in Figure 5.

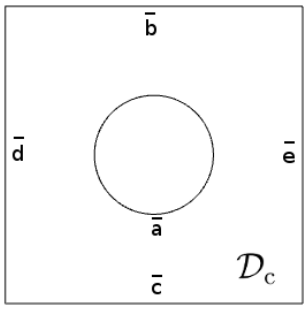


Figure 5 – Cloaking of a cylinder: geometry of $\mathcal{D}_{\mathrm{c}}$ and boundary definitions

Exploiting the properties of conformal transformations we get

$$\Lambda^{\mu}_{\bar{\mu}} = \begin{pmatrix} 1 & 0 & 0 & 0 \\ 0 & \frac{\partial y}{\partial \bar{y}} & -\frac{\partial y}{\partial \bar{x}} & 0 \\ 0 & \frac{\partial y}{\partial \bar{x}} & \frac{\partial y}{\partial \bar{y}} & 0 \\ 0 & 0 & 0 & 1 \end{pmatrix}, \qquad \Lambda^{\bar{\mu}}_{\mu} = \begin{pmatrix} 1 & 0 & 0 & 0 \\ 0 & \frac{\frac{\partial y}{\partial \bar{y}}}{\left(\frac{\partial x}{\partial \bar{x}}^2 + \frac{\partial x}{\partial \bar{y}}^2\right)} & \frac{\frac{\partial y}{\partial \bar{x}}}{\left(\frac{\partial x}{\partial \bar{x}}^2 + \frac{\partial x}{\partial \bar{y}}^2\right)} & 0 \\ 0 & \frac{-\frac{\partial y}{\partial \bar{x}}}{\left(\frac{\partial x}{\partial \bar{x}}^2 + \frac{\partial x}{\partial \bar{y}}^2\right)} & \frac{\frac{\partial y}{\partial \bar{y}}}{\left(\frac{\partial x}{\partial \bar{x}}^2 + \frac{\partial x}{\partial \bar{y}}^2\right)} & 0 \\ 0 & 0 & 0 & 1 \end{pmatrix} \tag{19}$$

This transformation maps the cylinder in a flat surface, leading to the loss of omnidirectionality. The compression of the cylinder cross–section into a point is obtainable with the solutions from the two Laplace's equations but, as previously said, coordinate lines would evidently no longer be locally orthogonal as the starting Cartesian are, Fig. 4.

In Figure 6, the obtained distribution of $\mathrm{c_R}/\mathrm{c_V}$ inside the cloak is presented, together with the coordinate mapping used $x = f_1(\bar{x}, \bar{y})$ and $y = f_2(\bar{x}, \bar{y})$. The cloaking capability of the designed device is evident in Figure 7, where the emitting point source is placed at y = 0. When the source is moved to y $\neq 0$, and the transformation is not changed accordingly, some scattering appears, Fig. 8: as said before, the cylinder is mapped into an horizontal line long as the original diameter.

As seen for carpet cloaking, it can be noted also in this application that some shift of the acoustic field is present. From a listener point of view, such a difference would not be noted, however, being the cloaked pressure field not identical to the incident one, the rigorous definition of acoustic cloaking is not completely satisfied.

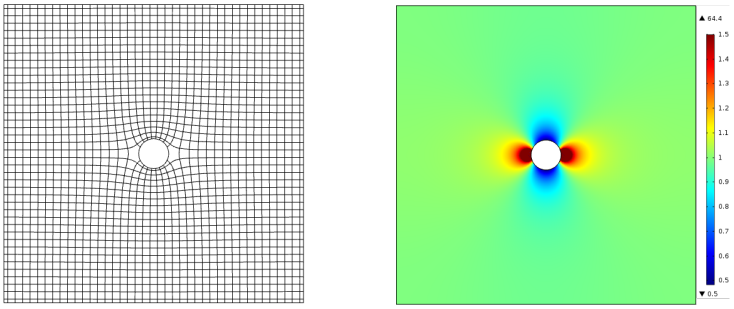

(a) Transformation (b) $c_R/c_V$

Figure 6 – Cloaking of a cylinder: coordinate transformation: $x = f_1(\bar{x}, \bar{y})$ and $y = f_2(\bar{x}, \bar{y})$ (a), Field distribution of $c_R/c_V$ inside $\mathcal{D}_c$(b)

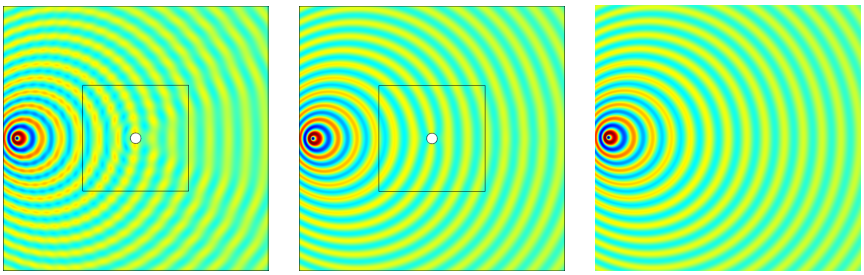

(a) Naked (b) Cloaked (c) Free Field

Figure 7 – Mass point source emitting at 655 Hz placed in y = 0 impinging on a naked cylinder (a), free field (b), cloaked cylinder (c), field visualization of Real part of acoustic potential $\mathrm{Re}(\phi)$.

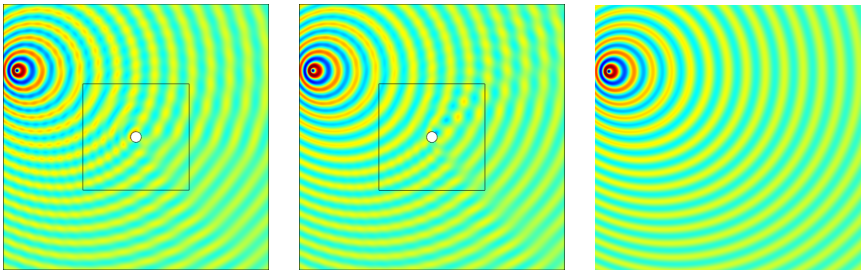

(a) Naked (b) Cloaked (c) Free Field

Figure 8 – Mass point source emitting at 655 Hz placed in y = 2.5 impinging on a naked cylinder (a), free field (b), cloaked cylinder (c), field visualization of Real part of acoustic potential $\mathrm{Re}(\phi)$.

## 4 ON CLOAKING EFFICIENCY

Efficiency tests on the cloaking capability of the device are carried out for the application presented in Section 3.2, varying the frequency of the incident acoustic field and the ratio between the surface occupied by the cylindrical object and the cloak surface.

It has been evidenced how the present metamaterial design method introduces a translation of the acoustic field between the free field case and in presence of the cloaked object, even when any reflection of the incident acoustic field by the object is suppressed. This consideration led to define a figure of merit $\sigma$ that considers the sound pressure level to evaluate efficiency and detect

any reflection by the cloaked object; in particular the absolute value of the difference between the pressure level in presence of the cloaked object and in free field conditions, integrated over the fluid domain is used.

$$\sigma = \int_{\mathcal{D}} |L_{\mathrm{p_{cloak}}} - L_{\mathrm{p_{free\,field}}}| \; d\mathcal{S} \tag{20}$$

where $L_{\mathrm{p}}$ is, as usual, $20 \log_{10} \left( \dfrac{\mathrm{p}}{\mathrm{p_{ref}}} \right)$, with $\mathrm{p_{ref}} = 20 \mu Pa$.

In Figure 9, values of $\sigma$ are reported for two frequencies (300 and 655 Hz, respectively) and different values of the surface ratio $\mathrm{S_{cloak}}/\mathrm{S_{object}}$. Analysing results, the efficacy of the device

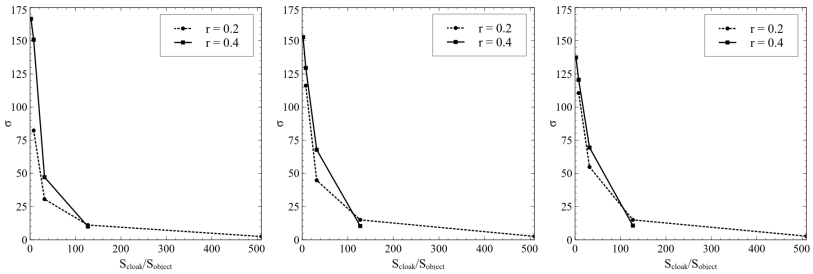


(a) 300Hz (b) 655Hz (c) 900Hz

Figure 9 – Values of $\sigma = \int_{\mathcal{D}} |L_{\mathrm{p_{cloak}}} - L_{\mathrm{p_{free\,field}}}| \; d\mathcal{S}$ for three test frequencies and two size of cloaked cylinder at various surface ratio $\mathrm{S_{cloak}}/\mathrm{S_{object}}$.

appears to be broadband, being the values of $\sigma$ in the same range for all three tested frequencies; however, it is also clear that a high value of the surface ratio $\mathrm{S_{cloak}}/\mathrm{S_{object}}$ is needed in order to obtain a significant scattering abatement effect, as can be seen by acoustic field visualizations of some of tested cases in Figures 10 and 11.

The need for such a large cloaking surface limits drastically the applicability of this design method in aeroacoustics especially in the aeronautical context, where size and weight constrains are critical.

## 5 ON CLOAK'S PERMEABILITY

The design methodology proposed in (4, 5) and recalled in this paper, considers a non–null velocity field inside the cloak domain $\mathcal{D}_{\mathrm{c}}$ to achieve the scattering cancellation in a moving fluid. This leads to an aerodynamically permeable cloak, and in this one is helped by the equality between the metamaterial and external fluid density.

However, analysing the velocity field arising from the (particular type of) quasi–conformal coordinate transformation used for both the carpet cloaking and the cylinder, it can be observed how this is different from the potential velocity field around the object to be cloaked; the latter could be in principle obtained, at least for aerodynamic bodies, with an aerodynamically permeable metamaterial, but the first is not achievable by a passive cloak as the velocity field is not physical.

In Figure 12 the two velocity fields are superimposed: in red the ATA–arising and in blue the potential velocity. Even though directions of velocity vectors of the two fields are substantially identical, the same can not be said for the modulus: the ATA velocity appears to have its maximum where the potential has its minimum and vice versa. This is due to the fact that the gradient of the solution of Eq. 13, from which the matrix $\Lambda^{\mu}_{\bar{\mu}}$ is built, follows the shape of the potential velocity, and the equivalence is exact when $\mathcal{D}_{\mathrm{cloak}}$ extends to infinity. However, the transformation matrix is its inverse $\Lambda^{\bar{\mu}}_{\mu}$, and this raises the question about how to obtain this velocity field.

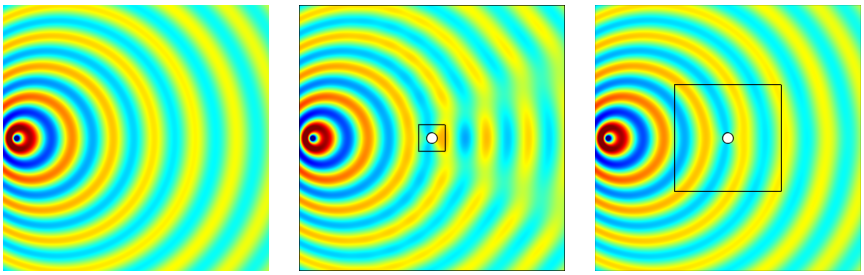

(a) FreeField

(b) $S_{cloak}/S_{object} \simeq 7$, r = 0.2

(c) $S_{cloak}/S_{object} \simeq 126$, r = 0.2

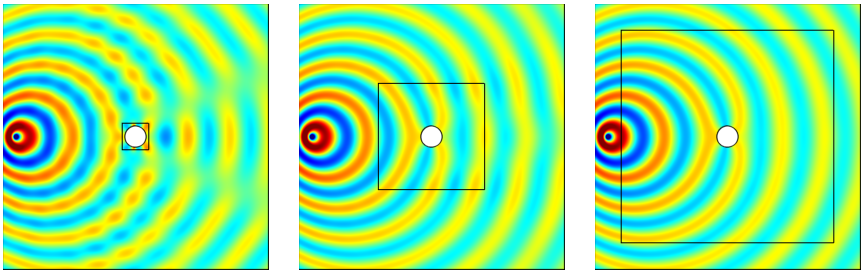

(d) $S_{cloak}/S_{object} \simeq 1$, r = 0.4

(e) $S_{cloak}/S_{object} \simeq 31$, r = 0.4

(f) $S_{cloak}/S_{object} \simeq 126$, r = 0.4

Figure 10 – Acoustic potential $\phi$ field visualization at 300 Hz: free field (a) is compared with a small (b and d) and a big (c, e and f) surface ratio configuration.

## 6 CONCLUSIONS

After a brief review of the Analogue Transformation Acoustics method, numerical simulations of two aeroacoustic scenarios are performed: a review on an assessed carpet cloaking application using ATA and quasi–conformal mapping and a new cloaking of a cylindrical object using ATA and conformal mapping that transforms the cylinder into a flat surface. In both cases ATA confirmed its ability to design a cloaking device operating in a moving fluid, *i.e.* in presence of a background uniform flow.

The so designed acoustic cloak fully recovers the wavefronts shape. A small phase shift is introduced in the acoustic field, especially in the zone behind the scattering object w.r.t. the incoming stream. The designed device appears to have broadband effect, but, unfortunately, needs an excessively large $S_{cloak}/S_{object}$ ratio to properly cancel scattering, too large specially for aeroacoustic applications where size and weight requirements are typically very stringent. To overcome the limitation of applicability of the method only to very small objects, a modification is needed in the way the coordinate transformation is obtained, for example extending the ATA approach to deal with anisotropy (using homogenization techniques or alternative analogue models) and hence removing the limitation to conformal transformations.

A deeper investigation on the velocity field requested inside the cloak domain evidences its non physical behaviour: this appears to be significantly different from a potential velocity field, having the first its maximum velocity magnitude where the latter has its minimum and vice–versa. A possible approach to overcome the difficulties that can arise from this can be to make use of the acoustic analogy to interpret the convective terms inside the cloak as equivalent acoustic sources, supposing a static fluid in this domain. Clearly, the criticality is moved to the practical realization of the acoustic analogy in this aerodynamically impermeable device, that is a non trivial task implying to achieve the pointwise control of the generation of acoustic sources and hence of the acoustic field, though in a small domain. A promising approach for its high spatial resolution could be the use of laser–generated sound source, as described in

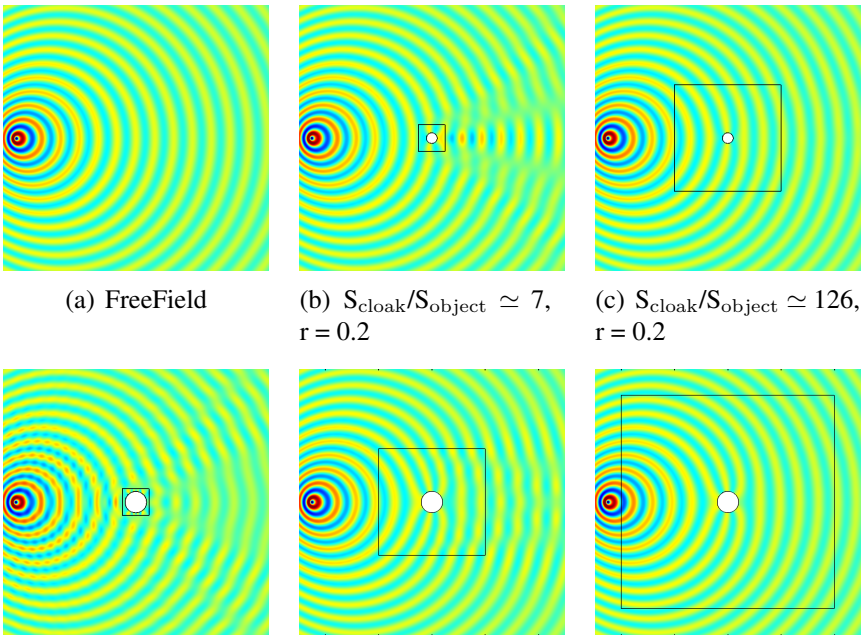

(a) FreeField

(b) $S_{cloak}/S_{object} \simeq 7$, r = 0.2

(c) $S_{cloak}/S_{object} \simeq 126$, r = 0.2

(d) $S_{cloak}/S_{object} \simeq 1$, r = 0.4

(e) $S_{cloak}/S_{object} \simeq 31$, r = 0.4

(f) $S_{cloak}/S_{object} \simeq 126$, r = 0.4

Figure 11 – Acoustic potential $\phi$ field visualization at 655 Hz: free field (a) is compared with a small (b and d) and a big (c, e and f) surface ratio configuration.

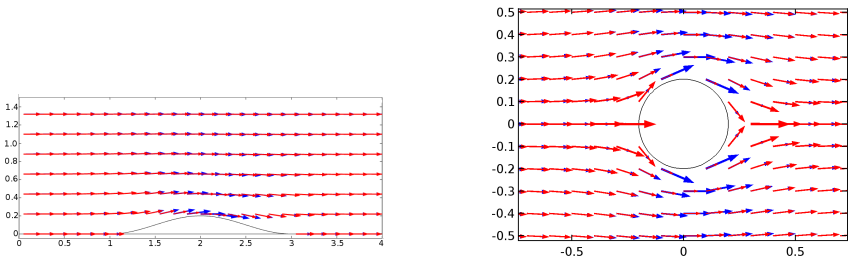

(a) Carpet cloaking

(b) Cloaking of a cylinder

Figure 12 – Comparison between the corrected ATA velocity field (red arrows) and the potential velocity field (blue arrows) around the bump (a) and the cylinder (b) inside $\mathcal{D}_c$

(19): focusing a high energy laser beam is possible to locally heat a very small volume of fluid creating a small plasma zone that, rapidly expanding, generates an omni-directional pressure wave that propagates at the isentropic speed of sound, *i.e.* a monopole point source.

## REFERENCES


1. Pendry J.B., Schurig D., Smith D.R. Controlling electromagnetic fields. Science (New York, NY) 2006, 312 (5781):1780–1782.

2. Cummer S.A., Schurig D. One path to acoustic cloaking. New Journal of Physics 2007, 9 (3):45.

3. García-Meca, C., Carloni, S., Barceló, C., Jannes, G., Sánchez-Dehesa, J., Martinez, A. Analogue Transformation Acoustics:An alternative theoretical framework for acous-

tic metamaterials, European Space Agency, the Advanced Concepts Team, Ariadna Final Report 2007:11-1301b.

4. García-Meca, C., Carloni, S., Barceló, C., Jannes, G., Sánchez-Dehesa, J., Martínez A. Analogue transformations in physics and their application to acoustics. Scientific reports 2013, 3, 2009.

5. García Meca, C., Carloni, S., Barceló, C, Jannes, G, Sánchez-Dehesa, J, Martinez, A. Supplementary Information : Analogue Transformations in Physics and their Application to Acoustics. Scientific reports 2013, 30.

6. García-Meca, C., Carloni, S., Barceló, C., Jannes, G., Sánchez-Dehesa, J., Martnez, A. Space-time transformation acoustics. Wave Motion 2014, 51 (5).

7. García-Meca, C., Carloni, S., Barceló, C., Jannes, G., Sánchez-Dehesa, J., and Martnez, A. Analogue transformation acoustics and the compression of spacetime. Photon Nanostruct: Fundam. Appl. 2014, http://dx.doi.org/10.1016/j.photonics.2014.05.001

8. Visser M. Acoustic propagation in fluids: An Unexpected example of Lorentzian geometry. arXiv:gr-qc/9311028.

9. Chang, Z., Zhou, X., Hu, J., & Hu, G. Design method for quasi-isotropic transformation materials based on inverse Laplace's equation with sliding boundaries. Opt. Express 2010 18 (6):6089–6096.

10. Hu, J., Zhou, X., & Hu, G. Design method for electromagnetic cloak with arbitrary shapes based on Laplace's equation. Opt. Express 2009, 17 (3):pp.1308–1320, https://doi.org/10.1364/OE.17.001308

11. Leonhardt U. Optical conformal mapping. Science (New York, NY) 2006, 312 (5781):1777–1780.

12. Norris A. N. Acoustic cloaking theory. Proceedings of the Royal Society A: Mathematical, Physical and Engineering Sciences 2008, 464 (2097):2411–2434.

13. Norris, A. N. Acoustic metafluids. The Journal of the Acoustical Society of America 2009, 125 (2):839–849.

14. Cai LW, Sánchez-Dehesa J. Analysis of Cummer–Schurig acoustic cloaking. New Journal of Physics 2007, 9 (12):450.

15. Torrent D, Sánchez-Dehesa J. Broadband acoustic cloaks based on the homogenization of layered materials. Wave Motion 2011, 48 (6):497–504.

16. Iemma U, Burghignoli L. An integral equation approach to acoustic cloaking. Journal of Sound Vibration 2012, 331:4629–4643.

17. Iemma U. Theoretical and Numerical Modeling of Acoustic Metamaterials for Aeroacoustic Applications. Aerospace 2016, 3 (2), 15 1-19.

18. Li, J., Pendry, J.B. Hiding under the Carpet: A New Strategy for Cloaking. Phys. Rev. Lett. 2008, 101 (20), 203901:1–4. https://link.aps.org/doi/10.1103/PhysRevLett.101.203901.

19. Rossignol K.S., Delfs J., Boden, F. On the Relevance of Convection Effects for a Laser–Generated Sound Source. Proc. 21st AIAA/CEAS Aeroacoustics Conference; 22-26 June 2015; Dallas; TX 2015.